Journal of Oral Biosciences 61 (2019) 163–172

Contents lists available at ScienceDirect

Journal of Oral Biosciences

journal homepage: www.elsevier.com/locate/job

Original Article

Porcine keratin 75 in developing enamel

Risako Chiba [a], Miu Okubo [b], Ryuji Yamamoto [a], Mari M. Saito [a], Saeko Kobayashi [c], Elia Beniash [d], Yasuo Yamakoshi [a, *]

[a] Department of Biochemistry and Molecular Biology, School of Dental Medicine, Tsurumi University, 2-1-3 Tsurumi, Tsurumi-ku, Yokohama 230-8501, Japan
[b] Department of Periodontology, School of Dental Medicine, Tsurumi University, 2-1-3 Tsurumi, Tsurumi-ku, Yokohama 230-8501, Japan
[c] Department of Pediatric Dentistry, School of Dental Medicine, Tsurumi University, 2-1-3 Tsurumi, Tsurumi-ku, Yokohama 230-8501, Japan
[d] Department of Oral Biology, University of Pittsburgh School of Dental Medicine, 3501 Terrace Street, Pittsburgh, PA 15261, USA

ARTICLE INFO

Article history:
Received 29 March 2019
Received in revised form
6 June 2019
Accepted 12 June 2019
Available online 26 June 2019

Keywords:
Tooth
Enamel
Amelogenesis
Keratin
Proteins

ABSTRACT

Objective: To provide *in vivo* biochemical evidence for the isolation, identification, and characterization of porcine keratin 75 (K75) in developing enamel.
Methods: Immunolocalization of K75 was observed in mandibles from mice at postnatal days 5 and 11. *K75* gene expression was analyzed by quantitative reverse transcription-polymerase chain reaction using enamel organ epithelium (EOE) of incisors from pigs at 5 months of age. Enamel protein was extracted and isolated from both immature and mature enamel of second molars from 5-month-old pigs, and the K75 antibody-positive fraction was analyzed by liquid chromatography-mass spectrometry (LC-MS/MS). *In vitro* protease digestion of K75-antibody-positive fraction was carried out using porcine kallikrein 4 (pKLK4) or recombinant human enamelysin (rhMMP20) and their degradation patterns were characterized by both SDS-PAGE and western blotting.
Results: Specific immunostaining for K75 was restricted to the layers of stratum intermedium and the enamel side of ameloblasts in mice at postnatal day 5, and to the papillary layer at postnatal day 11. Porcine *K75* was expressed throughout enamel formation, but its transcript levels were significantly higher in the transition EOE than in the secretory- and maturation-stage EOE. Porcine K75 was extracted from the neutral soluble fraction from both immature and mature enamel. It was identified by LC-MS/MS analysis, and was found not to be degraded by either pKLK4 or rhMMP20.
Conclusion: We propose that K75 is present in the developing enamel and undergoes different processing/degradation compared to other enamel proteins.

1. Introduction

Keratin is a major component of the stratum corneum of hair, nail, and skin, and is a salt-insoluble protein mainly involved in cellular structure formation. The keratin gene family has the greatest number of members in humans, with 54 distinct functional genes [1]. The keratin family is classified into two major groups, type I (acidic) and type II (neutral or basic), which assemble into heterodimers [2]. There are 28 type I keratin genes and 26 type II keratin genes, and at least 26 genes are specifically expressed in the hair follicle [1].

The type I and type II keratin gene subdomains are located on chromosomes 17 and 12, respectively [2]. Among the 54 keratin genes, approximately 21 genes including hair- and hair follicle-specific keratins are related to diverse hereditary disorders [3]. In hair diseases, mutations involving keratin 81, 83, and 86 (K81, K83, and K86) are associated with monilethrix, which is an autosomal dominant congenital condition that affects hair growth [4,5]. Of note, a single amino acid substitution (A161T) in K75 causes pseudofolliculitis barbae, which is a common disorder of the hair and skin [6]; it was found that dental enamel in individuals carrying

Abbreviations: Tris, tris(hydroxymethyl)aminomethane; EDTA, ethylenediaminetetraacetic acid; BSA, bovine serum albumin; DNA, deoxyribonucleic acid; RNA, ribonucleic acid; mRNA, messenger ribonucleic acid; SDS-PAGE, sodium dodecyl sulfate-polyacrylamide gel electrophoresis; Na_2HPO_4, disodium hydrogen phosphate; KH_2PO_4, potassium dihydrogen phosphate.

* Corresponding author. Fax: +81 45 573 9599.
E-mail addresses: chiba-r@tsurumi-u.ac.jp (R. Chiba), okubo-miu@tsurumi-u.ac.jp (M. Okubo), yamamoto-rj@tsurumi-u.ac.jp (R. Yamamoto), saito-mari@tsurumi-u.ac.jp (M.M. Saito), kinoshita-saeko@tsurumi-u.ac.jp (S. Kobayashi), ebeniash@pitt.edu (E. Beniash), yamakoshi-y@tsurumi-u.ac.jp (Y. Yamakoshi).

https://doi.org/10.1016/j.job.2019.06.002
1349-0079/

the pseudofolliculitis barbae-causing polymorphism, have altered enamel structure and mechanical properties, and are more susceptible to tooth decay [7]. In mature human enamel, K75 is found at the periphery of the enamel rods, where enamel rod sheaths are located [8]. These studies involving K75 in enamel have raised many questions regarding its roles and functional properties during amelogenesis.

Enamel formation progresses through three developmental stages: secretion, transition, and maturation. During these three stages, enamel proteins are secreted, proteolytically processed, degraded, and reabsorbed into ameloblasts [9,10]. The aims of this study were to investigate whether the cytosolic protein K75 is present in the enamel matrix, how it undergoes proteolytic processing and/or degradation, and what role it plays during enamel formation. Here, we provide *in vivo* biochemical evidence for the isolation, identification, and characterization of K75 in developing porcine enamel.

2. Materials and methods

2.1. Immunohistochemical analysis

Mandibles obtained from mice (Institute of Cancer Research, London, UK) at postnatal days 5 and 11 were dissected and fixed with 4% paraformaldehyde for 20 h at 4 °C. Hard tissues were decalcified at 4 °C in a 10% (w/v) Na_2-EDTA solution (pH 7.0) for 7 days and embedded in paraffin [11]. Formalin-fixed, paraffin-embedded mouse mandibles were sectioned with a microtome blade (A35; Feather Safety Razor Co., Osaka, Japan) on a sliding microtome (LS-113; Yamato-Kohki, Asaka, Japan) to produce 4.5 μm thick sections and were pretreated with 0.3% hydrogen peroxide for 40 min. The sections were treated with 10 mM Tris–EDTA solution (pH 9.0) for 5 min in a microwave for antigen retrieval, and incubated in a blocking solution (1% BSA, 10% normal goat serum) for 1 h at 23 °C. For primary antibody application, rabbit polyclonal anti-K75 antibody (#HPA019367; Atlas Antibodies AB, Bromma, Sweden) was used at a dilution of 1:500. For secondary antibody application, Histofine Simple Stain Mouse MAX-PO® antibody (#414341; Nichirei, Tokyo, Japan) was used without dilution. A positive signal was detected with 3,3′-diaminobenzidine (DAB) (TaKaRa, Kusatsu, Japan) as a staining substrate. Sections were counterstained to observe clear tissue and cell morphology after staining with haematoxylin. Light micrographs were obtained using a Canon EOS Kiss X8i camera (Tokyo, Japan) attached to an optical microscope (Olympus BX50, Tokyo, Japan).

2.2. Quantitative reverse transcription-polymerase chain reaction (RT-qPCR)

Enamel organ epithelium (EOE) at secretory and transition stages was dissected from the inner surface of the EOE. The EOE at the maturation stage was prepared from the labial surface of a 5-month-old porcine incisor in accordance with our previously reported methods [12]. RNA from the EOE samples at the three stages was extracted with RNA extraction reagent (Isogen, Nippon Gene Co., Ltd., Tokyo, Japan). Next, purified total RNA (2 μg) was reverse transcribed with Ready-To-Go You-Prime First-Strand Beads (GE Healthcare, Chicago, IL, USA); the reaction mixture consisted of SYBR Green PCR master mix (Roche Diagnostics GmbH, Mannheim, Germany), supplemented with 0.5 μM forward and reverse primers and 2 μL cDNA as template. After an initial preheating step at 95 °C for 10 min, samples were run for 45 cycles (denaturation for 10 s at 95 °C, annealing for 10 s at 60 °C and extension for 15 s at 72 °C). The specific primer sets were designed using Primer-BLAST software (http://www.ncbi.nlm.nih.gov/tools/primer-blast). The selected primers were K75-F (5′-CACGGCTGCCGAGAATGAAT-3′) paired with K75-R (5′-TGCTTCAAAGAGCATCCGCA-3′) to generate an amplified product of 133 bp. Glyceraldehyde-3-phosphate dehydrogenase (*GAPDH*) was used as a reference gene, and the selected primers were GAPDH-F (5′-CCATCACCATCTTCCAGGAG-3′) paired with GAPDH-R (5′-ACAGTCTTCTGGGTGGCAGT-3′) to generate an amplified product of 346 bp. Each ratio was normalized to the relative quantification data for *K75* in comparison with that of *GAPDH*, which was generated based on a mathematical model for relative quantification in qPCR systems. All values are presented as means ± standard error. Statistical significance was determined using Tukey–Kramer test; $p < 0.05$ was considered statistically significant.

2.3. Preparation and extraction of soft and hard enamel

EOE and dental pulp tissues were removed using tissue forceps. The soft (S), cheesy enamel and the hard (H), chalky enamel were separated from the crowns using a spatula. Both soft and hard enamel shavings were homogenized in 50 mM Na_2HPO_4/KH_2PO_4 buffer (pH 7.4) containing 5 mM dithiothreitol (DTT). The soluble fraction (N-extract) was collected by centrifugation for 10 min at 16,000 g.

2.4. Ammonium sulfate fractionation of porcine enamel proteins in the N-extract

N-extracts obtained from the S and H enamel were concentrated to 40% saturation by the addition of ammonium sulfate, and the precipitate (N1-S or N1-H) was removed by centrifugation. The supernatant was increased to 65% saturation and separated by centrifugation. The 40–65% saturation pellet was resuspended in 5 mL 0.5 M acetic acid, and the supernatants (N2-S and N2-H) and precipitates (N3-S and N3-H) were separated by centrifugation. All samples were characterized by SDS-PAGE and western blotting.

2.5. Identification of porcine K75 by mass spectrometry

The N2-S fraction (10 mg) containing K75 was fractionated by affinity high-performance liquid chromatography (HPLC) using a heparin Sepharose column (Tosoh, Tokyo, Japan) and eluted over a linear gradient (0%–100% buffer B in 50 min) at a flow rate of 0.4 mL/min. Buffer A comprised 50 mM Tris–HCl and 6 M urea (pH 7.4) with 5 mM DTT; buffer B comprised 50 mM Tris–HCl and 6 M urea (pH 7.4) with 5 mM DTT and 1 M NaCl. Protein was detected by optical absorbance at 280 nm. Fractions were collected every 2.5 min, and characterized by SDS-PAGE and western blotting. The protein content of each fraction was measured using a Pierce 660 nm protein assay kit (Thermo Scientific, Rockford, IL, USA) and samples were stored at −80 °C. Two K75 antibody positive protein bands were excised from SDS-PAGE gels. Liquid chromatography-mass spectrometry (LC-MS/MS) for these two proteins was performed by Japan Bio Service Co., Ltd. (Asaka, Saitama, Japan). Database searches were performed using the National Center for Biotechnology Information Protein database (http://www.ncbi.nlm.nih.gov/protein). The accession number of each keratin family member is shown in Appendix Table A1.

2.6. In vitro digestion of K75 by MMP20 and KLK4

For *in vitro* protease digestion of K75, recombinant human MMP20 (rhMMP20) was purchased from Enzo Life Sciences (Tokyo, Japan), and kallikrein 4 (pKLK4) was purified from porcine developing enamel based on our previously reported methods

[13]. The tenth fraction of the N2-S sample (50 μg) isolated by heparin-HPLC was dissolved in 45 μL 50 mM Tris–HCl containing 10 mM $CaCl_2$ and digested with rhMMP20 or pKLK4 (approximately 1 μg) for 20 h at 37 °C. Reaction aliquots at 0 and 20 h were characterized by western blotting. P148 amelogenin was used as a positive control and was characterized by SDS-PAGE after digestion.

2.7. SDS-PAGE and western blotting

SDS-PAGE was performed using a 5–20% gradient or a 15% e-PAGEL mini gel (Atto Corporation, Tokyo, Japan). Samples were dissolved in NuPAGE LDS sample buffer (Life Technologies/Invitrogen, Carlsbad, CA, USA) containing 2% β-mercaptoethanol, and electrophoresis was carried out at 30 mA for 60 min with Tris-glycine-SDS running buffer (Life Technologies/Invitrogen). The gel was stained with Simply Blue Safe Stain (Life Technologies/Invitrogen). The apparent molecular weights of the protein bands were estimated by comparison with SeeBlue Plus2 Pre-Stained Standard (Life Technologies/Invitrogen). A commercial antibody specific for human K75 was used (#ab39038; Abcam, Cambridge, MA, USA). Samples fractionated by SDS-PAGE were electrotransferred onto Invitrolon polyvinylidene difluoride membranes (Life Technologies/Invitrogen). Samples were incubated with K75 antibody overnight (1:1,000 dilution) at 4 °C. The secondary antibody (#172-1019, horseradish peroxidase-conjugated goat anti-rabbit IgG, BioRad, Hercules, CA, USA) was diluted 1:5,000 followed by incubation for 1 h at 23 °C. Immunopositive bands were visualized by chemiluminescent detection using the ECL Advance Western Blotting Detection Kit (GE Healthcare). Full images from SDS-PAGE and western blotting that were cropped in the main figures are shown in Appendix Fig. A1.

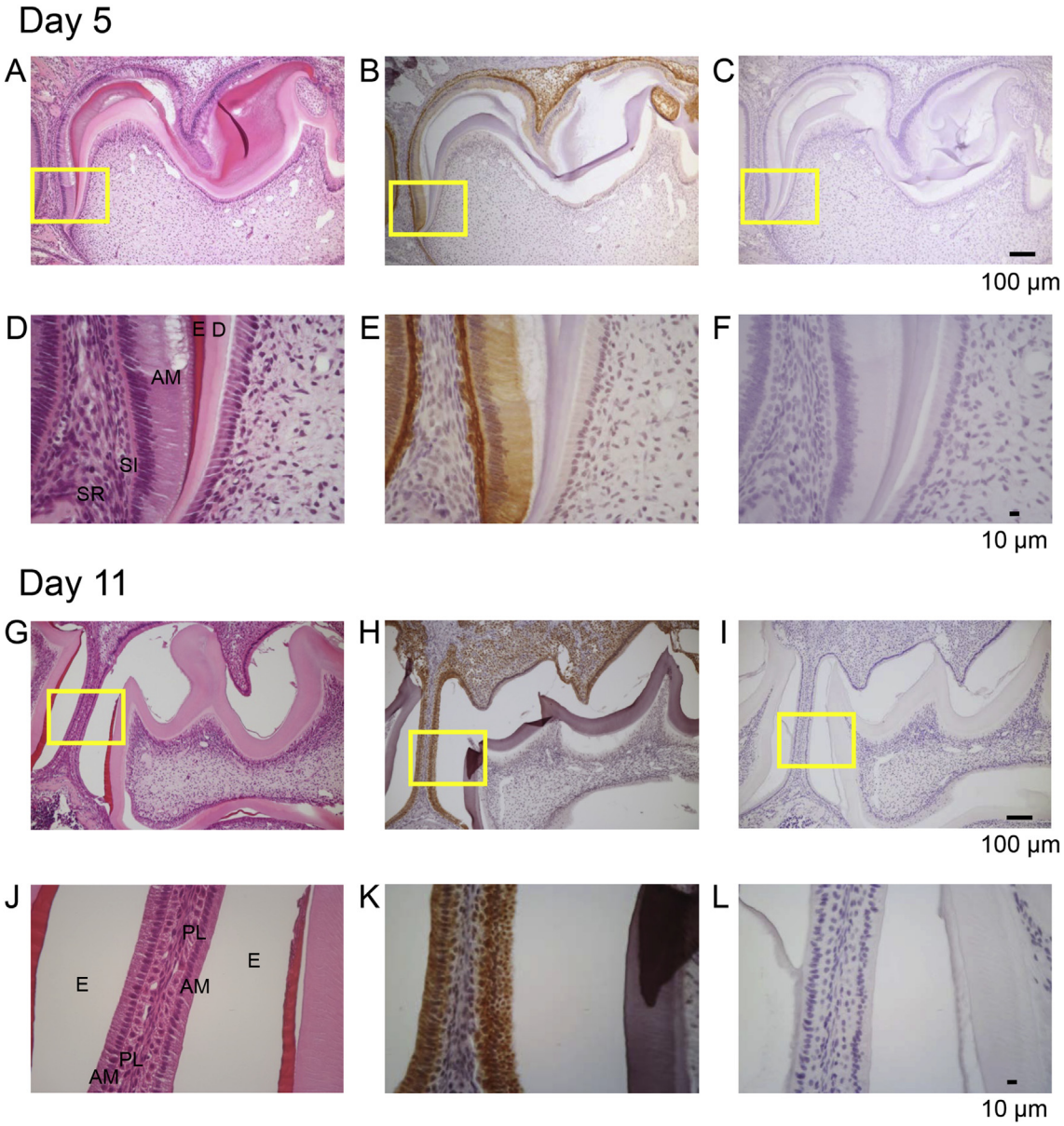

Fig. 1. Immunohistochemical detection of keratin 75 from the first molar enamel organ of mice at postnatal days 5 and 11. (A, D, G, J) Haematoxylin and eosin staining, **(B, E, H, K)** anti-keratin 75 antibody, and **(C, F, I, L)** absence of primary antibody as a control. **(A–C** and **G–I)** Magnification 100×. **(D-–F** and **J–L)** Magnification 400×; these images are a higher magnification of the boxed areas. SR, stellate reticulum; SI, stratum intermedium; PL, papillary layer; AM, ameloblast; E, enamel; D, dentin.

2.8. Densitometry

Positive bands against the K75 antibody on western blotting were quantified using ImageJ software (US National Institutes of Health, Bethesda, MD, USA).

3. Results

3.1. Immunohistochemical detection of mouse K75 from molar tooth germ

We first investigated the locations of K75 in mouse enamel organ. First molar tooth germ sections in the developing mouse were immunostained using antibodies against mouse K75 (Fig. 1). Specific immunostaining for K75 was restricted to the layers of the stratum intermedium and the enamel side of ameloblasts in mice at postnatal day 5, and to the papillary layer at postnatal day 11.

3.2. Gene expression of porcine K75 during enamel formation

After determining that K75 was localized in mouse enamel organ during amelogenesis, we conducted further studies in the pig model to identify K75 in enamel at the protein level. For this purpose, we first investigated the expression of porcine *K75* at the genetic level. We prepared total RNA isolated from EOE corresponding to the secretory, transition, and maturation stages (Fig. 2A). qPCR analysis revealed that *K75* mRNA expression levels were approximately 2.25–4.50-fold higher in the transition EOE than in secretory or maturation EOE (Fig. 2B).

3.3. Extraction of porcine K75 in enamel matrix

Using our previously reported methods [14], porcine enamel matrix in S or H enamel was extracted under neutral (N) conditions. The N-extracts were further fractionated into three fractions: ammonium sulfate precipitate (ASP) at 40% saturation (N1), 40–65% ASP soluble in acid (N2), and 40–65% ASP insoluble in acid (N3). SDS-PAGE showed that neutral soluble amelogenin, such as P103 (13 kDa) from the S enamel, was extracted in N1-S, whereas albumin from both S and H enamel was fractionated in N3-S and N3-H (Fig. 2C). Western blotting with an anti-K75 antibody revealed that K75 was mostly fractionated in N2-S and N2-H (Fig. 2D). The intensity of the major K75 band at approximately 55 kDa in N2-H decreased modestly to approximately 80% of that in N2-S (Fig. 2E).

The N2-S-extracts were subjected to HPLC using a heparin column. Using this method, the extracts were fractionated into 20 fractions (Fig. 3A), and SDS-PAGE (Fig. 3B) and western blotting (Fig. 3C) showed that K75 mainly eluted in the 8th to 11th fractions. We excised a K75 antibody-positive gel protein band that migrated at approximately 55 kDa in the 8th to 9th fractions, and proteins were identified using LC-MS/MS. LC-MS/MS analysis yielded seven peptide sequences in porcine K75 (Fig. 3D): ^{155}TLNNKFASFIDK^{166}, ^{169}FLEQQNKVLETK^{180}, ^{313}SLDLDSIIAEVK^{324}, ^{325}AQYEDIANRSR^{333}, ^{334}AEAESWYQTK^{345}, ^{346}YEELQVTAGR^{355}, and ^{441}LALDVEIATYR^{452}.

3.4. Identification of porcine K75 in enamel matrix

In order to compare pig and human type II keratins, we created a multiple sequence alignment and investigated the consistency of the amino acid sequence of seven K75 peptides identified in the LC-MS/MS analysis. Compared with K75, other porcine type II keratins exhibited at least one mismatched amino acid (Fig. 4). Total consistency calculated from the total number of amino acids of seven peptides and the number of mismatched amino acids was 57.9%–94.7% against porcine K75 (Fig. 4). Of note, the consistency of K80, K81, K83, and K85 was remarkably low.

We further investigated the consistency of seven peptides against human type II keratins (Fig. 5). On comparing pig and human K75 peptides, the peptide sequence of porcine S^{313}-K^{324} showed homology to N^{313}-K^{324} in human K75. Apart from this peptide, the remaining six peptide sequences were consistent

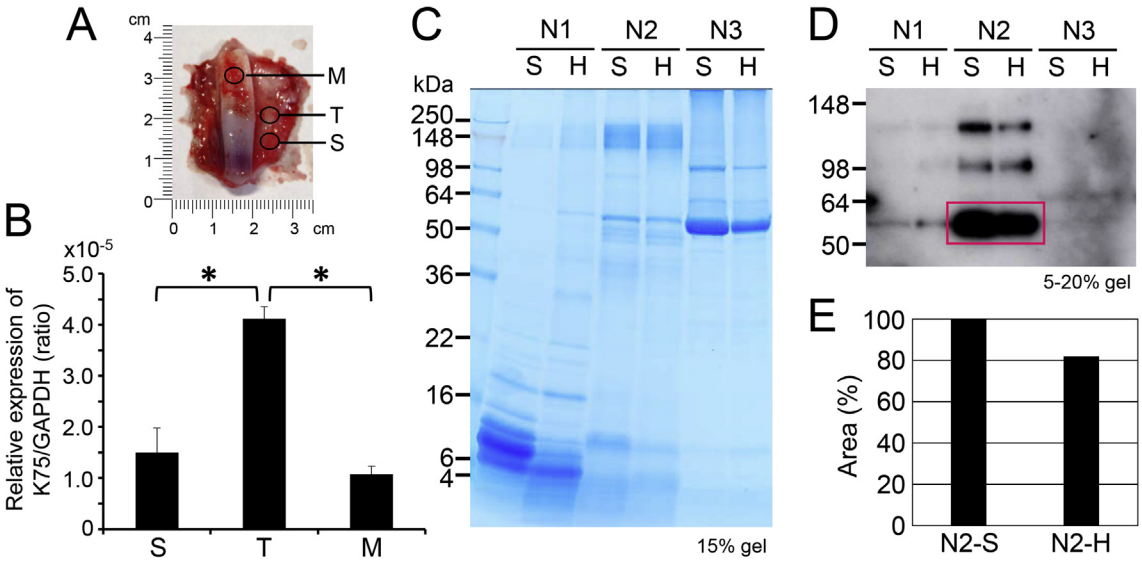

Fig. 2. Expression of keratin 75 gene in porcine enamel organ epithelium and detection of keratin 75 protein in porcine developing enamel. (A) Permanent incisor and enamel organ epithelium (EOE) from a 5-month-old pig. The secretory (S)-, transition (T)- and maturation (M)-stage ameloblast layers were excised with a razor blade. **(B)** The mRNA expression of keratin 75 (*K75*) in S-, T- and M-stage ameloblasts. Ratios were normalized to a reference gene (*GAPDH*) (n = 6 ameloblasts at each stage). **(C)** SDS-PAGE (15% gel) stained with Simply Blue Safe Stain and **(D)** western blotting (5%–20% gel) using a specific antibody against K75, showing the neutral soluble extracts from soft (S) and hard (H) enamel fractionated by ammonium sulfate precipitation. N1, ammonium sulfate precipitate (ASP) at 40% saturation; N2, 40%–65% ASP soluble in acid; N3, 40%–65% ASP insoluble in acid. **(E)** Quantification of K75 antibody-positive bands indicated by a red square in D. The area of each band on western blotting was determined using ImageJ software and normalized relative to the density of the N2-S band.

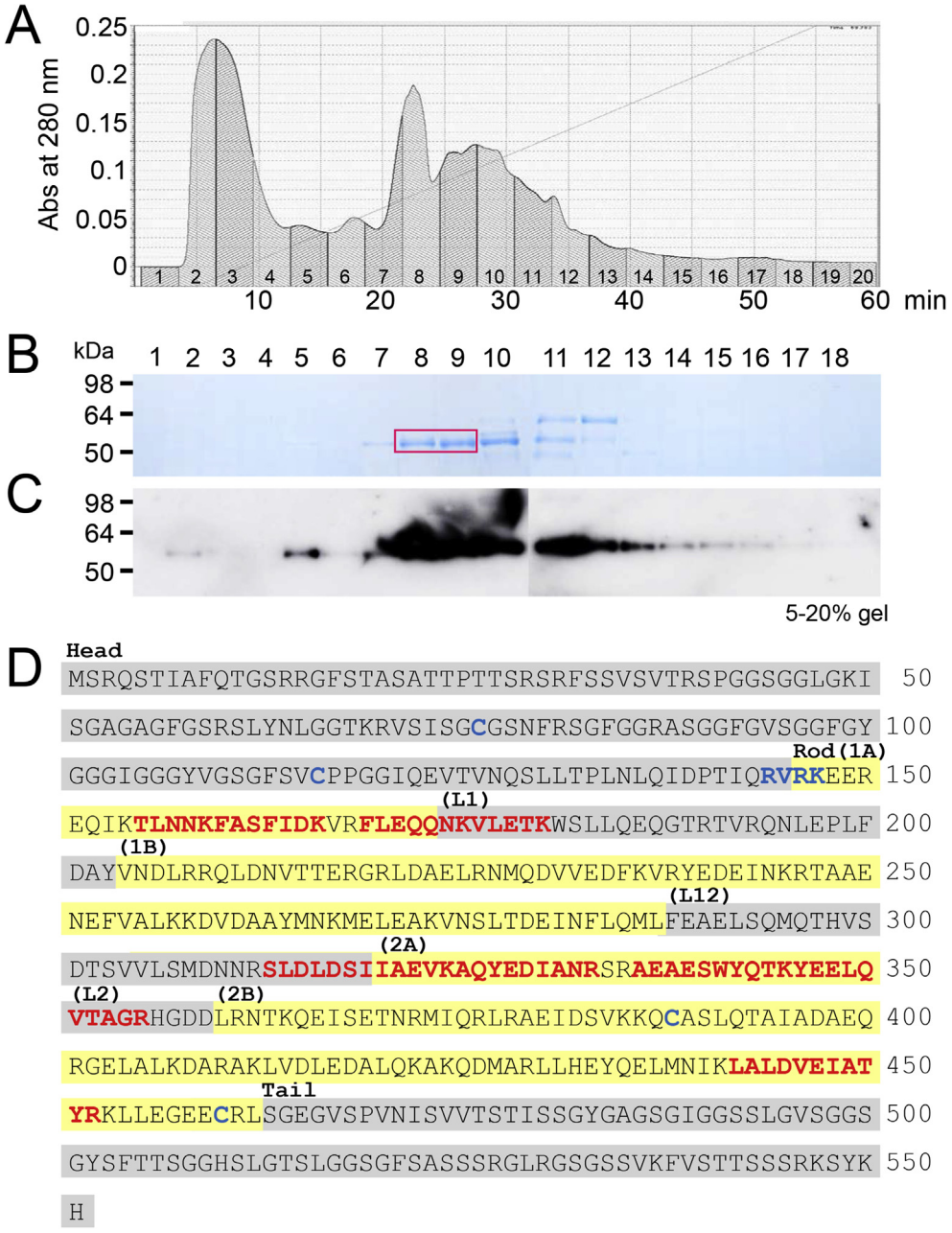

Fig. 3. Isolation and identification of keratin 75 protein in porcine developing enamel. (A) Heparin HPLC chromatogram showing absorbance at 280 nm for the N2-S sample (10 mg). Twenty fractions were collected at 2.5 min intervals each. **(B)** SDS-PAGE gel (5%–20% gel) stained with Simply Blue Safe Stain and **(C)** western blotting (5%–20% gel) using a specific antibody against K75 showing fractions 1 to 20 on heparin HPLC chromatogram. **(D)** Amino acid sequence of porcine K75. Three structural domains are indicated as Head, Rod, and Tail. The rod regions are further divided into seven subdomains: α-helical central rod domains (1A, 1B, 2A, and 2B) (yellow) and linker domains (L1, L12, and L2) (grey). The number of the last amino acid in each row is provided on the right. Amino acid sequences identified by LC-MS/MS analysis for K75 antibody-positive bands (red frame in B) are indicated in red. Four cysteines and the consensus amino acid sequence for the heparin-binding site are indicated in blue. (For interpretation of the references to colour in this figure legend, the reader is referred to the Web version of this article.)

between the two species. Other human type II keratins contained at least one different amino acid compared with porcine K75. The overall consistency of human type II keratins against porcine K75 was 53.9%–98.7% (Fig. 5).

3.5. *In vitro digestion of K75 by MMP20 and KLK4*

The intensities of the K75 bands in the N2-S and N2-H fractions were almost equal by western blotting analysis (Fig. 2D); therefore, we investigated whether K75 was affected by KLK4 and/or MMP20. The K75 fraction isolated by heparin-HPLC was digested with pKLK4 or rhMMP20. Both SDS-PAGE and western blotting showed that K75 bands were almost unchanged before and after digestion with pKLK4 or rhMMP20 (Fig. 6A and B). We further determined the change in the area of each band before and after digestion (Fig. 6C). The pKLK4 band at 20 h decreased to approximately 20% of the baseline level (0 h), whereas the rhMMP band at 20 h was decreased by only 7%. Porcine 25 kDa (P173) amelogenin was also digested as a control (Fig. 6D and E). Both pKLK4 and rhMMP20 markedly degraded P173 amelogenin (approximately 72% for pKLK4 and nearly 100% for rhMMP20), which reduced the apparent sizes of this protein to approximately 13 and

```
K1    187 SLNNQFASFIDK 198  201 FLEQQNQVLQTK 212  345 HLDLNSIIDEVK 356  357 AQYEEIAQR 365
K2    195 TLNNKFACFIDK 206  209 FLEQQNQVLKTK 220  353 NLDLNDIISEVQ 364  365 SQYEEIAHR 373
K3    209 TLNNKFASFIDK 220  223 FLEQQNKVLETK 234  369 FLDLDSIIAEVK 380  381 AQYEEIAQR 389
K4    152 ILNDKFASFIDK 163  166 FLEQQNKVLETK 177  310 DLDLDSIIAEVR 321  322 AQYEEITQR 330
K5    179 TLNNKFASFIDK 190  193 FLEQQNKVLDTK 204  337 NLDLDSIIAEVK 348  349 AQYEDIANR 357
K8    105 TLNNKFASFIDK 116  119 HLEQQNKVLETK 130  261 SLDLDGIIAEVK 272  273 AQYEEIANR 281
K71   138 ALNNKFASFIDK 149  152 FLEQQNQVLETK 163  296 DLNLDSIIDEVR 307  308 AQYEEIALK 316
K72   142 ALNNKFASFIDK 153  156 FLEQQNQVLETK 167  300 DLDLDSIIAEVR 311  312 AQYEDISLK 320
K73   138 ALNNKFASFIDK 149  152 FLEQQNQVLETK 163  296 SLDLDSIIAEVQ 307  308 AQYEEIALK 316
K74   146 ALNNKFASFIDK 157  160 FLEQQNQVLETK 171  304 DLDLDSIIAEVR 315  316 AQYEDIALK 324
K75   155 TLNNKFASFIDK 166  169 FLEQQNKVLETK 180  313 SLDLDSIIAEVK 324  325 AQYEDIANR 333
K77   172 VLNNKFASFIDK 183  186 FLEQQNQVLQTK 197  330 SLDLDSIIDAVR 341  342 TQYELIAQK 350
K78   146 TLNNQFASFIDK 157  160 FLEQQNQVLQTK 171  304 RLDFRDIIAEVR 315  316 ARYEEITRT 324
K79   148 TLNDKFASFIDK 159  162 FLEQQNKVLETK 173  308 NLDLDSIIAEVK 319  320 AQYEQIAQR 328
K80   165 ALNDKFASLIGK 176  179 ALEQRNQLLETR 190  321 HLDLSGIVEEVK 332  333 AQYDAIAAR 341
K81   112 CLNNRFAAFIDK 123  126 FLEQQNKLLETK 137  268 DLNMDNIVAEIK 279  280 AHYDDIASR 288
K82   124 CLNNRFASFINK 135  138 FLEQKNKLLETK 149  280 ELDVDGIIAEIK 291  292 AQYDEIASR 300
K83   117 CLNNRFAAFIDK 128  131 FLEQQNKLLETK 142  273 DLNMNNIVAEIK 284  285 AQYDDIASR 293
K84   173 TLNNKFASFIDK 184  187 FLEQQNKLLETK 198  329 DLNVDGIIADIK 340  341 AQYEEIARR 349
K85   129 NLNSRFAAFIDK 140  143 FLEQQNKLLETK 154  285 DLNMNXVVAEIK 296  297 AQYDDVASR 305

K1    368 AEAETLYQSK 377  378 YEELQITAGQ 387  474 LALDVEIATYR 484  (81.6)
K2    376 AEAEALYHSK 385  386 YEELQITAGK 395  482 LALDVEIATYR 492  (77.6)
K3    392 AEAEALYQTK 401  402 LGELQTTAGR 411  498 LALDVEIATYR 508  (89.5)
K4    333 AEAEALYQIK 342  343 IQQLQISVDQ 352  439 LALDIEIATYR 449  (75.0)
K5    360 TEAESWYQTK 369  370 YEELQQTAGR 379  466 LALDVEIATYR 476  (94.7)
K8    284 AEAETMYQIK 293  294 YEELQSLAGK 303  390 LALDVEIATYR 400  (88.2)
K71   319 AEAEALYQTK 328  329 FQELQLAAGR 338  425 LALDMEIATYR 435  (78.9)
K72   323 AEAEALYQSK 332  333 IQELQVTAGQ 342  429 LALDVEIATYR 439  (82.9)
K73   319 AEAEALYQTK 328  329 FQELQLAAGQ 338  425 LALDIEIATYR 435  (81.6)
K74   327 AEAEALYQSK 336  337 IQELQLAAGQ 346  433 LALDMEIATYR 443  (80.3)
K75   336 AEAESWYQTK 345  346 YEELQVTAGR 355  441 LALDVEIATYR 451  (100)
K77   353 EEAEALYQTK 362  363 YQELQITAGR 372  459 LSLDVEIATYR 469  (80.3)
K78   327 AEAEMLYQTK 336  337 YQELQVSAQL 346  433 LALDVEIATYR 443  (76.3)
K79   331 AEAEAWYQSK 340  341 YEELQVTAGK 350  437 LALDVEIATYR 447  (92.1)
K80   344 EEAEAYSRSQ 353  354 LEERAACSAE 363  450 LALDVEIATYR 460  (57.9)
K81   291 AEAESWYRSK 300  301 CEEIKATVVR 310  397 LGLDIEIATYR 407  (69.7)
K82   303 AEAEAWYQGR 312  313 YEELRLTAGN 322  409 LGLDIEIATYR 419  (73.7)
K83   296 AEAESWYRSK 305  306 CEEIKATVVR 315  402 LGLDIEIATYR 412  (69.7)
K84   352 ADAESWYQTK 361  362 YEEMRVTAGQ 371  458 LALDIEIATYR 468  (81.6)
K85   308 AEAESWYRSK 317  318 CEEMKATVVR 327  414 LGLDIEIATYR 424  (65.8)
```

Fig. 4. Multiple sequence alignment of porcine type II keratins. The first and last numbers of each peptide indicate the position in each keratin (K). K75 peptides identified by LC-MS/MS analysis are surrounded by a black frame. The mismatched amino acid against K75 peptides is represented in red. The unknown amino acid in peptide D^{285}-K^{296} of K85 is indicated by the blue "x". Numbers in parentheses indicate consistency when K75 was set to 100%. (For interpretation of the references to colour in this figure legend, the reader is referred to the Web version of this article.)

5 kDa for rhMMP20 and several cleavage products for pKLK4, respectively.

4. Discussion

An immunohistochemical study in rats showed that keratins were strongly localized in stratum intermedium cells of developing incisor enamel organs [15]. In a recent study, it was demonstrated that K75 is present in secretory-stage ameloblasts [7]. In the present study, we observed that K75 is localized in stratum intermedium cells and on the side of the enamel in ameloblasts in the first molar in mice at day 5 (secretory stage). Our findings are consistent with these previous reports.

At the maturation stage, cells in contact with the base of ameloblasts change to the shape of the papillary layer, and stratum intermedium cells disappear [16]. Immunostaining using a pan-keratin antibody has shown that the papillary layer forms a keratin-like network of epithelial strands between tooth crowns and oral epithelium [17]. We demonstrated that in mice, K75 is distributed throughout the papillary layer in the first molar at day 11 (early maturation stage). This finding suggested that K75 is also a constituent of papillary layer cells and stratum intermedium cells.

An SV40-immortalized porcine ameloblast-like cell line has been established and characterized [18], but no information is available regarding *K75* gene expression. We have previously succeeded in isolating total RNA from EOE corresponding to the secretory, transition, and maturation stages [12]. As shown in Fig. 2A, the secretory-stage ameloblasts are separated from the enamel layer along with the rest of the EOE in the permanent incisors of 5-month-old pigs. In contrast, maturation-stage ameloblasts adhere to the underlying enamel layer because the basement membrane of maturation-stage ameloblasts mediates the attachment of these epithelial cells to the mineralized tooth surface. Using this technique, we demonstrated that the *K75* transcript was expressed throughout the amelogenesis process, although its mRNA expression level in transition-stage EOE was significantly

K75(P)	155	TLNNKFASFIDK	166	169	FLEQQNKVLETK	180	313	SLDLDSIIAEVK	324	325	AQYEDIANR	333
K1	186	SLNNQFASFIDK	197	200	FLEQQNQVLQTK	211	344	SLDLDSIIAEVK	355	356	AQNEDIAQK	364
K2	184	TLNNKFASFIDK	195	198	FLEQQNQVLQTK	209	342	NLDLDSIIAEVK	353	354	AQYEEIAQR	362
K3	176	TLNNKFASFIDK	187	190	FLEQQNKVLETK	201	336	SLDLDSIIAEVR	347	348	AQYEDIAQR	356
K4	231	LLNNKFASFIDK	242	245	FLEQQNKVLETK	256	389	NLDLDSIIAEVR	400	401	AQYEEIAQR	409
K5	174	TLNNKFASFIDK	185	188	FLEQQNKVLDTK	199	332	NLDLDSIIAEVK	343	344	AQYEEIANR	352
K6	138	VLNNKFASFIDK	149	152	FLEQQNQVLETK	163	296	NLDLDSIIAEVR	307	308	AQYEEIARK	316
K7	97	TLNNKFASFIDK	108	111	FLEQQNKLLETK	122	254	SLDLDGIIAEVK	265	266	AQYEEMAKC	274
K8	97	TLNNKFASFIDK	108	111	FLEQQNKMLETK	122	253	SLDMDSIIAEVK	264	265	AQYEDIANR	273
K71	136	ALNNKFASFIDK	147	150	FLEQQNQVLETK	161	294	NLDLDSIIDEVR	305	306	TQYEEIALK	314
K72	131	ALNNKFASFIDK	142	145	FLEQQNQVLETK	156	289	DLDLDSIIAEVR	300	301	AQYEEIALK	309
K73	138	VLNNKFASFIDK	149	152	FLEQQNQVLETK	163	296	NLDLDSIIAEVR	307	308	AQYEEIARK	316
K74	146	VLNDKFASFIDK	157	160	FLEQQNQVLETK	171	304	DLDLDSIIAEVR	315	316	MHYEEIALK	324
K75	155	TLNNKFASFIDK	166	169	FLEQQNKVLETK	180	313	NLDLDSIIAEVK	324	325	AQYEDIANR	333
K76	189	TLNNKFASFIDK	200	203	FLEQQNKVLETK	214	347	CLDLGSIIAEVR	358	359	AQYEEIAQR	367
K77	170	VLNNKFASFIDK	181	184	FLEQQNQVLQTK	195	328	SLDLDSIIDAVR	339	340	TQYELIAQR	348
K78	117	TLNNQFASFIDK	128	131	FLEQQNKVLETK	142	275	YLDFSSIITEVR	286	287	ARYEEIARS	295
K79	148	TLNNKFASFIDK	159	162	FLEQQNKVLETK	173	308	NLDLDSIIAEVK	319	320	AQYELIAQR	328
K80	89	ALNDKFASLIGK	100	103	ALEQRNQLLETR	114	245	HIDLSGIVEEVK	256	257	AQYDAVAAR	265
K81	112	SLNSRFAAFIDK	123	126	FLEQQNKLLETK	137	268	DLNMDCIIAEIK	279	280	AQYDDIVTR	288
K82	126	CLNNRFASFINK	137	140	FLEQKNKLLETK	151	282	ELDVDGIIAEIK	293	294	AQYDDIASR	302
K83	117	SLNSRFAAFIDK	128	131	FLEQQNKLLETK	142	273	DLNMDCMVAEIK	284	285	AQYDDIATR	293
K84	171	TLNNKFASFIDK	182	185	FLEQQNKLLETK	196	327	DLNLDGIIAEVK	338	339	AQYEEVARR	347
K85	129	SLNSRFAAFIDK	140	143	FLEQQNKLLETK	154	285	DLNMDCIIAEIK	296	297	AQYDDVASR	305
K86	112	SLNSRFAAFIDK	123	126	FLEQQNKLLETK	137	268	DLNMDCIIAEIK	279	280	AQYDDIVTR	288

K75(P)	334	AEAESWYQTK	343	344	YEELQVTAGR	353	441	LALDVEIATYR	451	(100)
K1	367	AEAESLYQSK	376	377	YEELQITAGR	386	473	LALDLEIATYR	483	(85.5)
K2	365	EEAEALYHSK	374	375	YEELQVTVGR	384	471	LALDVEIATYR	481	(85.5)
K3	359	AEAEALYQTK	368	369	LGELQTTAGR	378	465	LALDVEIATYR	475	(90.8)
K4	412	AEAEALYQTK	421	422	VQQLQISVDQ	431	518	LALDIEIATYR	528	(78.9)
K5	355	TEAESWYQTK	364	365	YEELQQTAGR	374	461	LALDVEIATYR	471	(93.4)
K6	319	AEAEALYQTK	328	329	FQELQLAAGR	338	425	LSLDIEIATYR	435	(80.3)
K7	277	AEAEAWYQTK	286	287	FETLQAQAGK	296	383	LALDIEIATYR	393	(82.9)
K8	276	AEAESMYQIK	285	286	YEELQSLAGK	295	382	LALDIEIATYR	392	(89.5)
K71	317	AEAEALYQTK	326	327	FQELQLAAGR	336	423	LALDMEIATYR	433	(78.9)
K72	312	AEAETLYQTK	321	322	IQELQVTAGQ	331	418	LALDMEIATYR	428	(82.9)
K73	319	AEAEALYQTK	328	329	FQELQLAAGR	338	425	LSLDIEIATYR	435	(80.3)
K74	327	AEAEALYQTK	336	337	IQELQLAASR	346	433	LALDMEIATYR	443	(76.3)
K75	336	AEAESWYQTK	345	346	YEELQVTAGR	355	442	LALDVEIATYR	452	(98.7)
K76	370	SEAEALYQTK	379	380	LGELQTTAGR	389	476	LALDVEIATYR	486	(85.5)
K77	351	DEAEALYQTK	360	361	YQELQITAGR	370	457	LSLDVEIATYR	467	(80.3)
K78	298	AEAEALYQTK	307	308	YQELQVSAQL	317	404	LSLDVEIATYR	414	(77.6)
K79	331	AEAEAWYQTK	340	341	YEELQVTAGK	350	437	LALDVEIATYR	447	(93.4)
K80	268	EEAEAYSRSQ	277	278	LEEQAARSAE	287	374	LALDIEIATYR	384	(53.9)
K81	291	AEAESWYRSK	300	301	CEEMKATVIR	310	397	LGLDIEIATYR	407	(69.7)
K82	305	AEAEAWYQCR	314	315	YEELRVTAGN	324	411	LGLDIEIATYR	421	(76.3)
K83	296	AEAESWYRSK	305	306	CEEMKATVIR	315	402	LGLDIEIATYR	412	(68.4)
K84	350	ADAEAWYQTK	359	360	YEEMQVTAGQ	369	456	LGLDIEIATYR	466	(82.9)
K85	308	AEAESWYRSK	317	318	CEEMKATVIR	327	414	LGLDIEIATYR	424	(69.7)
K86	291	AEAESWYRSK	300	301	CEEMKATVIR	310	397	LGLDIEIATYR	407	(69.7)

Fig. 5. Multiple sequence alignment of human type II keratins. The first and last numbers of each peptide indicate the position in each keratin (K). Porcine K75 peptides identified by LC-MS/MS analysis (K75(P)) and human K75 (K75) are surrounded by a black frame. The mismatched amino acid against porcine K75 peptides is represented in red. Numbers in parentheses indicate the consistency when porcine K75 is set to 100%. (For interpretation of the references to colour in this figure legend, the reader is referred to the Web version of this article.)

higher than in both secretory- and maturation-stage EOE. These findings at the genetic level led us to further investigate K75 in enamel at the protein level.

We have previously established a comprehensive strategy for isolating and purifying porcine enamel proteins [14]. We used this method to identify K75 protein in the enamel of pigs rather than mice because of the advantage of a larger tooth size. Hard keratins, such as those found hair and nail, are generally insoluble in water and organic solvents due to their high cysteine content (up to 18% in some hair) and high degree of crosslinking [19]. However, keratins are less resistant to oxidizing and reducing agents that interfere with their main stabilizing bonds (i.e., disulfide bridges) [20,21]. We demonstrated the extraction of K75 in developing enamel in a neutral buffer containing DTT. Considering that K75 contains only 0.7% cysteine, as shown in Table 1, our finding may suggest that K75 was solubilized in the extraction buffer with relative ease in the presence of oxidizing and reducing agents.

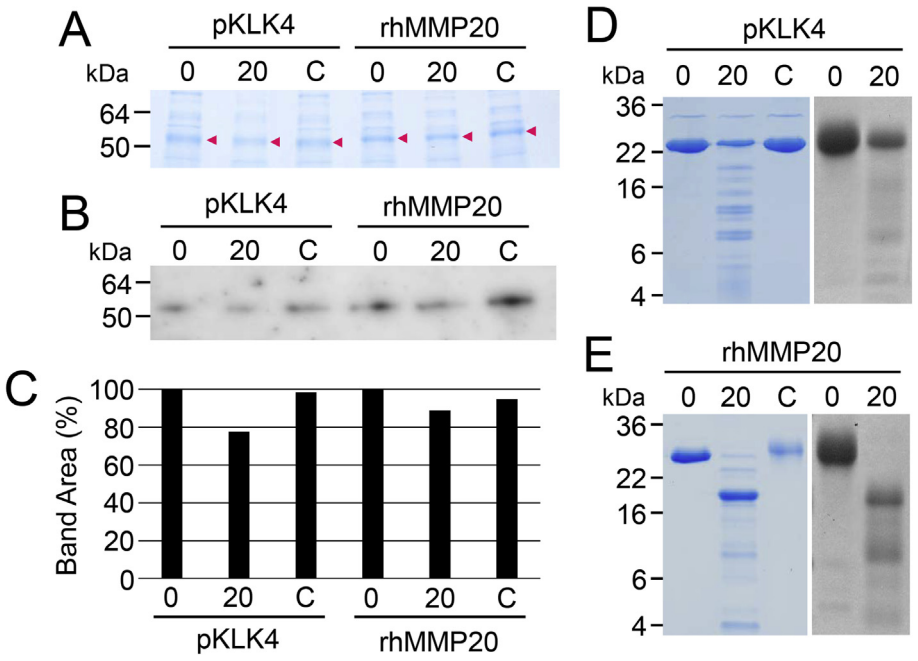

Fig. 6. *In vitro* digestion of porcine keratin 75 by MMP20 or KLK4. Porcine keratin (K)75 fraction isolated by heparin-HPLC and porcine amelogenin (p173 amelogenin) were incubated with pKLK4 or rhMMP20 for 0 and 20 h, respectively. **(A)** SDS-PAGE (5–20% gel) stained with Simply Blue Safe Stain showing the porcine K75 fraction. **(B)** Western blotting (5%–20% gel) using a specific antibody against K75 showing the porcine K75 fraction. **(C)** The area of each K75 band on SDS-PAGE (arrowhead in **(A)**) was determined using ImageJ software and normalized relative to the density of the 0 h band. **(D and E)** SDS-PAGE (15% gel) stained with Simply Blue Safe Stain showing the amelogenin fraction before and after digestion (i.e., positive control). C, incubation without pKLK4 or rhMMP20. (For interpretation of the references to colour in this figure legend, the reader is referred to the Web version of this article.)

Although we were able to detect K75 bands in S and H enamel by western blotting, our main aim was to determine the origin of this cytosolic protein. A number of unconventional secretory pathways involving cytosolic proteins have been reported [22–27], but the mechanisms underlying these trafficking pathways remain unclear. Moreover, because there is an abundance of keratin on the surface of the human body, it is important to consider the possibility of contamination, despite working on a clean bench and wearing disposable clothing (coat, gloves, cap, and mask). In other words, the possibility of contamination with other keratin family members from a location other than enamel during the process of sample preparation, extraction, and isolation must be considered. To eliminate this possibility, we directly analyzed a partial sequence of protein detected by K75 antibody.

Table 1
Amino acid composition of porcine K75, sheath proteins, tuft protein, albumin, and immunoglobulin heavy chain.

	Porcine	Porcine Sheath Proteins[a]			Tuft	Porcine
	K75	17K	15K	13K	Protein[b]	Albumin[c]
Ala	67	38	17	0	62	86
Arg	73	38	43	36	29	45
Asn	42	19	26	24	73	22
Asp	47	19	0	0		65
Cys	7	0	0	0	0	60
Gln	49	140	148	167	115	34
Glu	71	45	26	24		103
Gly	111	76	87	71	182	27
His	9	25	35	48	32	31
Ile	42	32	17	24	20	39
Leu	87	89	104	83	78	107
Lys	51	25	26	36	29	98
Met	18	38	35	36	16	0
Phe	36	51	52	60	39	50
Pro	15	166	157	167	131	51
Ser	120	83	96	95	82	39
Thr	64	32	43	36	46	45
Trp	4	13	17	24	0	3
Tyr	25	13	17	24	43	38
Val	64	57	52	48	29	57

Values represent numbers of amino acid residues per 1,000 total residues.
[a] Calculated from amino acid sequence (Chun et al., 2010; Iwata et al., 2007).
[b] (Robinson, Lowe, & Weatherell, 1975).
[c] Calculated from the deduced amino acid sequence (Accession: AY663543.1).

For this purpose, we needed to further purify K75 for LC-MS/MS analysis. Certain consensus peptide sequences have been proposed for heparin-binding proteins, such as BBXB or BXBB, where B denotes a basic amino acid residue [28]. As shown in Fig. 3D, we found that K75 possesses one heparin-binding site (R^{144}-K^{147}) in the head domain. Based on this finding, we were able to isolate K75 in the N2-S fraction on a heparin affinity HPLC column.

In-gel digestion has been widely used for proteome analysis [29–32]. The high detection sensitivity of mass spectrometry allows for detection of small amounts of keratin. In order to minimize contamination with keratin other than K75, we excised a protein band on an SDS-PAGE gel and transferred it to an autoclaved tube on a clean bench while wearing disposable clothing (see above).

All keratins possess the common protein structural characteristics of three domains: head, rod and tail. A central rod domain composed of approximately 310 amino acids comprises subdomains 1A, 1B, 2A, and 2B connected by linkers L1, L12, and L2 [33–35]. We confirmed that seven partial amino acid sequences obtained from LC-MS/MS analysis exist in the central rod domain of K75. As this region exhibits 70–80% homology among keratin molecular species [36], we were easily able to compare the amino acid sequences of the entire keratin family. We demonstrated that the amino acid sequence of seven K75 peptides obtained after LC-MS/MS analysis contained at least one mismatched amino acid with other porcine and all human type II keratins. These results suggested that K75 exists in porcine enamel, and that our results are not due to contamination.

During amelogenesis, the processing and degradation of enamel proteins progress through the action of two proteases: MMP20 [37] and KLK4 [38]. Enamel proteins are slowly processed by MMP20 to provide space within the deeper enamel matrix to allow the enamel crystallites to grow wider and thicker during the secretory stage, whereas they are progressively degraded by KLK4 within the enamel matrix so the enamel crystallites can grow wider and thicker during the transition and maturation stages [39–41]. Unlike these enamel proteins, keratin is generally inaccessible to common proteases, and only certain types of proteases such as keratinases are able to accomplish the degradation of keratin [42]. We identified only approximately 18% degradation of K75 from S enamel to H enamel, as shown in Fig. 2E. Moreover, our *in vitro* results demonstrated that K75 was hardly degraded by either pKLK4 or rhMMP20. These results suggest that in contrast to other enamel proteins, K75 in enamel may not be susceptible to enamel proteases. Moreover, considering that the amount of K75 is not increased in H enamel, as shown in Fig. 2D, the transportation of K75 by unconventional secretory pathways probably occurs mainly during the secretory stage.

K75 is detected in the rod sheaths and tufts of mature human enamel [7,8]. We have previously reported that MMP20-generated 13 kDa and 15 kDa cleavage products of porcine ameloblastin N-terminal region were immunolocalized in prism sheaths in enamel [43–45]. The immunoreactivity of these sheath proteins has also been detected in filamentous structures closely related to enamel sheaths in the enamel tuft [46]. Moreover, it has been reported that the enamel tuft contains an extremely insoluble protein termed "tuft protein" [47] and serum-derived albumin [48]. Western blotting showed that tuft protein and human skin keratin cross-react with proteins (molecular weight range 50–70 kDa) from demineralized developing enamel, enamel organ, human skin, and tuft extract [49]. We confirmed that the amino acid composition of K75 was different from that of the 13 kDa and 15 kDa sheath proteins, tuft protein, and albumin, as shown in Table 1. Further studies are needed to investigate the relationship between K75 and other enamel proteins.

In conclusion, we propose that K75 is present in developing enamel and undergoes a different form of processing/degradation as compared to other enamel proteins.

Ethical approval

All experimental procedures involving the use of animals were reviewed and approved by the Institutional Animal Care Committee and the Recombinant DNA Experiment and Biosafety Committee of the Tsurumi University School of Dental Medicine. Tooth germs of permanent molars and permanent incisors were surgically extracted for protein and genetic experiments, respectively, from the mandibles of 5-month-old pig cadavers obtained from the Meat Market of the Metropolitan Central Wholesale Market (Shinagawa, Tokyo, Japan).

Conflicts of interests

The authors declare no potential conflicts of interest with respect to the authorship and/or publication of this article.

CRediT authorship contribution statement

Risako Chiba: Conceptualization, Data curation, Formal analysis, Investigation, Writing - original draft. **Miu Okubo:** Data curation, Formal analysis, Investigation. **Ryuji Yamamoto:** Data curation, Formal analysis, Investigation. **Mari M. Saito:** Formal analysis. **Saeko Kobayashi:** Formal analysis. **Elia Beniash:** Conceptualization, Investigation. **Yasuo Yamakoshi:** Conceptualization, Data curation, Formal analysis, Investigation, Resources, Writing - original draft, Writing - review & editing.

Acknowledgements

We thank Dr. Yoshinobu Asada from the Department of Pediatric Dentistry and Dr. Ichiro Saito from the Department of Pathology at the School of Dental Medicine, Tsurumi University, Yokohama, Japan, for their support. This study was supported by a JSPS KAKENHI Grant-in-Aid for Scientific Research (C) (18K09627 and 17K11975) and the MEXT-Supported Program for the Strategic Research Foundation at Private Universities (S1511018).

Appendix A. Supplementary data

Supplementary data to this article can be found online at https://doi.org/10.1016/j.job.2019.06.002.

References

[1] Schweizer J, Bowden PE, Coulombe PA, Langbein L, Lane EB, Magin TM, et al. New consensus nomenclature for mammalian keratins. J Cell Biol 2006;174:169–74.
[2] Moll R, Divo M, Langbein L. The human keratins: biology and pathology. Histochem Cell Biol 2008;129:705–33.
[3] Chamcheu JC, Siddiqui IA, Syed DN, Adhami VM, Liovic M, Mukhtar H. Keratin gene mutations in disorders of human skin and its appendages. Arch Biochem Biophys 2011;508:123–37.
[4] Schweizer J, Langbein L, Rogers MA, Winter H. Hair follicle-specific keratins and their diseases. Exp Cell Res 2007;313:2010–20.
[5] Winter H, Rogers MA, Langbein L, Stevens HP, Leigh IM, Labreze C, et al. Mutations in the hair cortex keratin hHb6 cause the inherited hair disease monilethrix. Nat Genet 1997;16:372–4.
[6] Winter H, Schissel D, Parry DA, Smith TA, Liovic M, Birgitte Lane E, et al. An unusual Ala12Thr polymorphism in the 1A α-helical segment of the companion layer-specific keratin K6hf: evidence for a risk factor in the etiology of the common hair disorder pseudofolliculitis barbae. J Investig Dermatol 2004;122:652–7.
[7] Duverger O, Ohara T, Shaffer JR, Donahue D, Zerfas P, Dullnig A, et al. Hair keratin mutations in tooth enamel increase dental decay risk. J Clin Investig 2014;124:5219–24.
[8] Duverger O, Beniash E, Morasso MI. Keratins as components of the enamel organic matrix. Matrix Biol 2016;52-54:260–5.
[9] Smith CE, Pompura JR, Borenstein S, Fazel A, Nanci A. Degradation and loss of matrix proteins from developing enamel. Anat Rec 1989;224:292–316.
[10] Smith CE, Nanci A. Protein dynamics of amelogenesis. Anat Rec 1996;245:186–207.
[11] Gao Y, Li D, Han T, Sun Y, Zhang J. TGF-beta1 and TGFBR1 are expressed in ameloblasts and promote MMP20 expression. Anat Rec 2009;292:885–90 (Hoboken, NJ : 2007).
[12] Kobayashi-Kinoshita S, Yamakoshi Y, Onuma K, Yamamoto R, Asada Y. TGF-β1 autocrine signalling and enamel matrix components. Sci Rep 2016;6:33644.
[13] Yamakoshi Y, Hu JC-C, Fukae M, Iwata T, Simmer JP. How do MMP-20 and KLK4 process the 32 kDa enamelin? Eur J Oral Sci 2006;114(Suppl. 1):45–51.
[14] Yamakoshi Y, Hu JC-C, Ryu OH, Tanabe T, Oida S, Fukae M, et al. A comprehensive strategy for purifying pig enamel proteins. In: Kobayashi I, Ozawa H, editors. Biomineralization: formation, diversity, evolution and application proceedings of the 8th international symposium on biomineralization, niigata, Jpn, sept 25-28, 2001. Hadano, Jpn: Tokai University Press; 2003. p. 326–32.
[15] Nakai M, Tatemoto Y, Mori H, Mori M. Distribution profiles of keratin proteins during rat amelogenesis. Histochemistry 1986;85:89–94.
[16] Kallenbach E. Cell architecture in the papillary layer of rat incisor enamel organ at the stage of enamel maturation. Anat Rec 1967;157:683–8.
[17] Liu H, Yan X, Pandya M, Luan X, Diekwisch TG. Daughters of the enamel organ: development, fate, and function of the stratum intermedium, stellate reticulum, and outer enamel epithelium. Stem cells and development; 2016.
[18] DenBesten PK, Gao C, Li W, Mathews CH, Gruenert DC. Development and characterization of an SV40 immortalized porcine ameloblast-like cell line. Eur J Oral Sci 1999;107:276–81.
[19] Kasperova A, Kunert J, Raska M. The possible role of dermatophyte cysteine dioxygenase in keratin degradation. Med Mycol 2013;51:449–54.
[20] Horvath AL. Solubility of structurally complicated materials: 3. Hair. Sci World J 2009;9:255–71.
[21] Hill P, Brantley H, Van Dyke M. Some properties of keratin biomaterials: Kerateines. Biomaterials 2010;31:585–93.
[22] Nickel W, Rabouille C. Mechanisms of regulated unconventional protein secretion. Nat Rev Mol Cell Biol 2008;10:148.

[23] Rabouille C, Malhotra V, Nickel W. Diversity in unconventional protein secretion. J Cell Sci 2012;125:5251–5.
[24] Boya P, Reggiori F, Codogno P. Emerging regulation and functions of autophagy. Nat Cell Biol 2013;15:713–20.
[25] Rabouille C. Pathways of unconventional protein secretion. Trends Cell Biol 2017;27:230–40.
[26] Grieve AG, Rabouille C. Golgi bypass: skirting around the heart of classical secretion. Cold Spring Harb Perspect Biol 2011;3.
[27] Nickel W. The mystery of nonclassical protein secretion. A current view on cargo proteins and potential export routes. Eur J Biochem 2003;270:2109–19.
[28] Shimazaki K, Uji K, Tazume T, Kumura H, Shimo-Oka T. Approach to identification and comparison of the heparin-interacting sites of lactoferrin using synthetic peptides. Excerpta Med Int Congr Ser 2000;1195:37–46.
[29] Rosenfeld J, Capdevielle J, Guillemot JC, Ferrara P. In-gel digestion of proteins for internal sequence analysis after one- or two-dimensional gel electrophoresis. Anal Biochem 1992;203:173–9.
[30] Borchers C, Peter JF, Hall MC, Kunkel TA, Tomer KB. Identification of in-gel digested proteins by complementary peptide mass fingerprinting and tandem mass spectrometry data obtained on an electrospray ionization quadrupole time-of-flight mass spectrometer. Anal Chem 2000;72:1163–8.
[31] Shevchenko A, Tomas H, Havlis J, Olsen JV, Mann M. In-gel digestion for mass spectrometric characterization of proteins and proteomes. Nat Protoc 2006;1:2856–60.
[32] Granvogl B, Ploscher M, Eichacker LA. Sample preparation by in-gel digestion for mass spectrometry-based proteomics. Anal Bioanal Chem 2007;389:991–1002.
[33] Lane EB, McLean WH. Keratins and skin disorders. J Pathol 2004;204:355–66.
[34] Parry DA, Strelkov SV, Burkhard P, Aebi U, Herrmann H. Towards a molecular description of intermediate filament structure and assembly. Exp Cell Res 2007;313:2204–16.
[35] Ku NO, Gish R, Wright TL, Omary MB. Keratin 8 mutations in patients with cryptogenic liver disease. N Engl J Med 2001;344:1580–7.
[36] Steinert PM, Roop DR. Molecular and cellular biology of intermediate filaments. Annu Rev Biochem 1988;57:593–625.
[37] Bartlett JD, Simmer JP, Xue J, Margolis HC, Moreno EC. Molecular cloning and mRNA tissue distribution of a novel matrix metalloproteinase isolated from porcine enamel organ. Gene 1996;183:123–8.
[38] Simmer JP, Ryu OH, Qian Q, Zhang C, Cao X, Sun X, et al. Cloning and characterization of a cDNA encoding human EMSP1. In: Goldberg M, Boskey A, Robinson C, editors. Chemistry and biology of mineralized tissues: proceedings of the sixth international conference, Vittel, France, 1998. Vittel, France: American academy of orthopaedic surgeons, 6300 north river Rd, Rosemont, IL, 60018 USA; 1998. p. 205–8.
[39] Fukae M, Yamamoto R, Karakida T, Shimoda S, Tanabe T. Micelle structure of amelogenin in porcine secretory enamel. J Dent Res 2007;86:758–63.
[40] Lu Y, Papagerakis P, Yamakoshi Y, Hu JC, Bartlett JD, Simmer JP. Functions of KLK4 and MMP-20 in dental enamel formation. Biol Chem 2008;389:695–700.
[41] Smith CE. Cellular and chemical events during enamel maturation. Crit Rev Oral Biol Med 1998;9:128–61.
[42] Navone L, Speight R. Understanding the dynamics of keratin weakening and hydrolysis by proteases. PLoS One 2018;13:e0202608.
[43] Iwata T, Yamakoshi Y, Hu JC, Ishikawa I, Bartlett JD, Krebsbach PH, et al. Processing of ameloblastin by MMP-20. J Dent Res 2007;86:153–7.
[44] Chun YH, Yamakoshi Y, Yamakoshi F, Fukae M, Hu JC, Bartlett JD, et al. Cleavage site specificity of MMP-20 for secretory-stage ameloblastin. J Dent Res 2010;89:785–90.
[45] Hu CC, Fukae M, Uchida T, Qian Q, Zhang CH, Ryu OH, et al. Sheathlin: cloning, cDNA/polypeptide sequences, and immunolocalization of porcine enamel sheath proteins. J Dent Res 1997;76:648–57.
[46] Amizuka N, Uchida T, Nozawa-Inoue K, Kawano Y, Suzuki A, Li M, et al. Ultrastructural images of enamel tufts in human permanent teeth. J Oral Biosci 2005;47:33–41.
[47] Robinson C, Hudson J. Tuft protein: protein cross-linking in enamel development. Eur J Oral Sci 2011;119(Suppl 1):50–4.
[48] Ito Y. Acetic acid insoluble fraction obtained from porcine deciduous molar tooth enamel-characterization of proteins contained in enamel tufts. Tsurumi Univ Dent J 1998;24:235–47.
[49] Robinson C, Shore RC, Kirkham J. Tuft protein: its relationship with the keratins and the developing enamel matrix. Calcif Tissue Int 1989;44:393–8.